

1. Introduction

The thermal electron population characteristics in the transition region between the inner magnetosphere and magnetotail are of special interest because this region can be considered as a source of the electrons which end up in the radiation belts, accelerated up to several MeV. We present an empirical model of the electron temperature and density on the nightside for geocentric distances $r = 6-11 R_E$. The model is constructed using measurements onboard THEMIS probes during geomagnetic storms in 2010-2013. We use the data of ESA and SST detectors in the energy range from tens eV to 300-keV. The total size of the dataset is equivalent to ~400 hours of the observations in the plasma sheet complemented by the observations in the solar wind. The model outputs the electron temperature and density in the equatorial plane as a function of coordinate and interplanetary medium parameters.

2. Data

Data selection:

- THEMIS A, D, E probes
- The probes are in the central part of the plasma sheet $|B_z| > |B_r|$
- Storm-time intervals 2007-2013
- SYM-H < -50, 1 day before, 1 day after

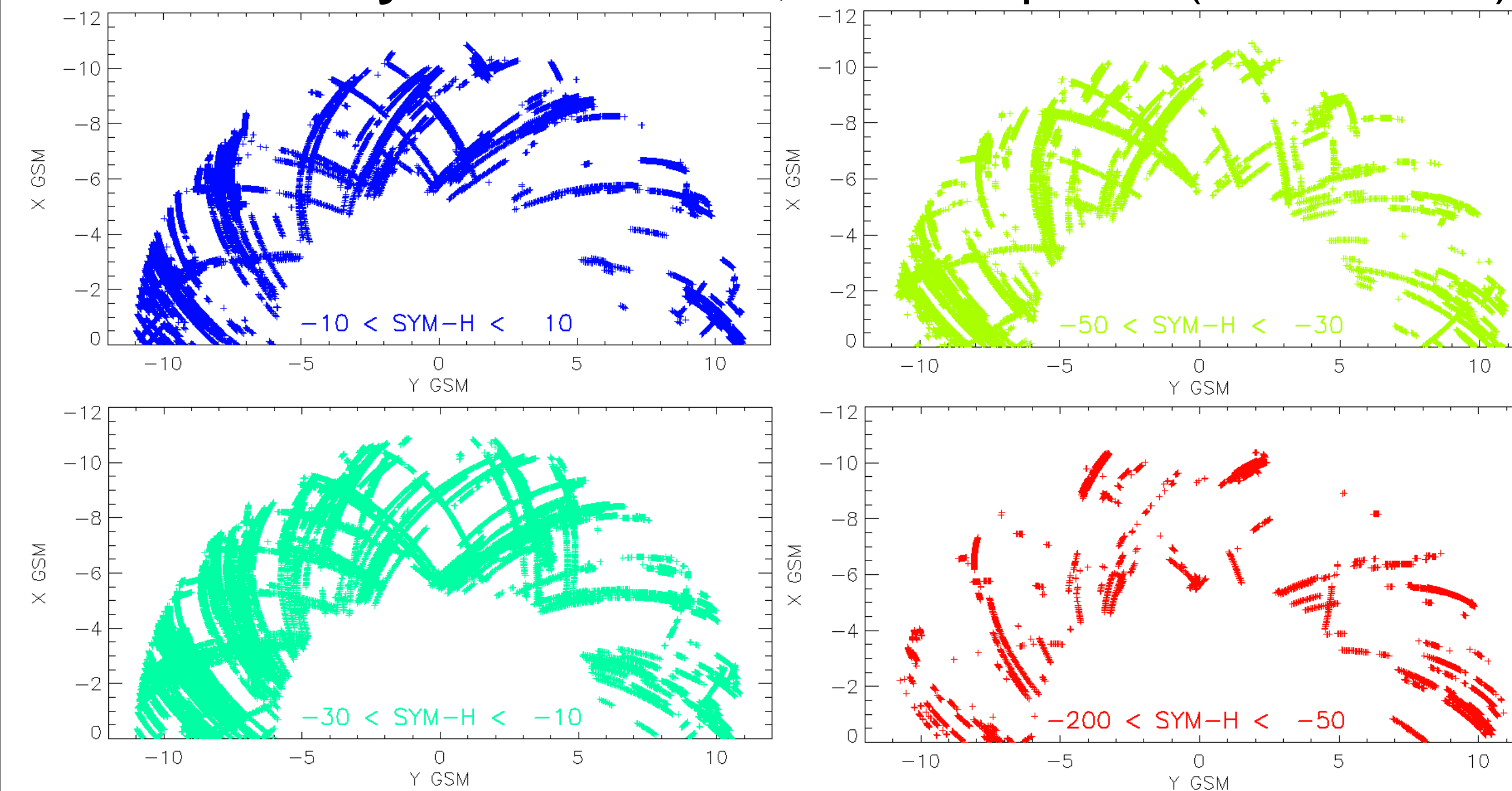
Plasma moments:

ESA electrons: 30eV - 30 keV;
 ions: 30eV - 25 keV
 SST ions and electrons ~25 keV - 300 keV

N_i = N_e test:

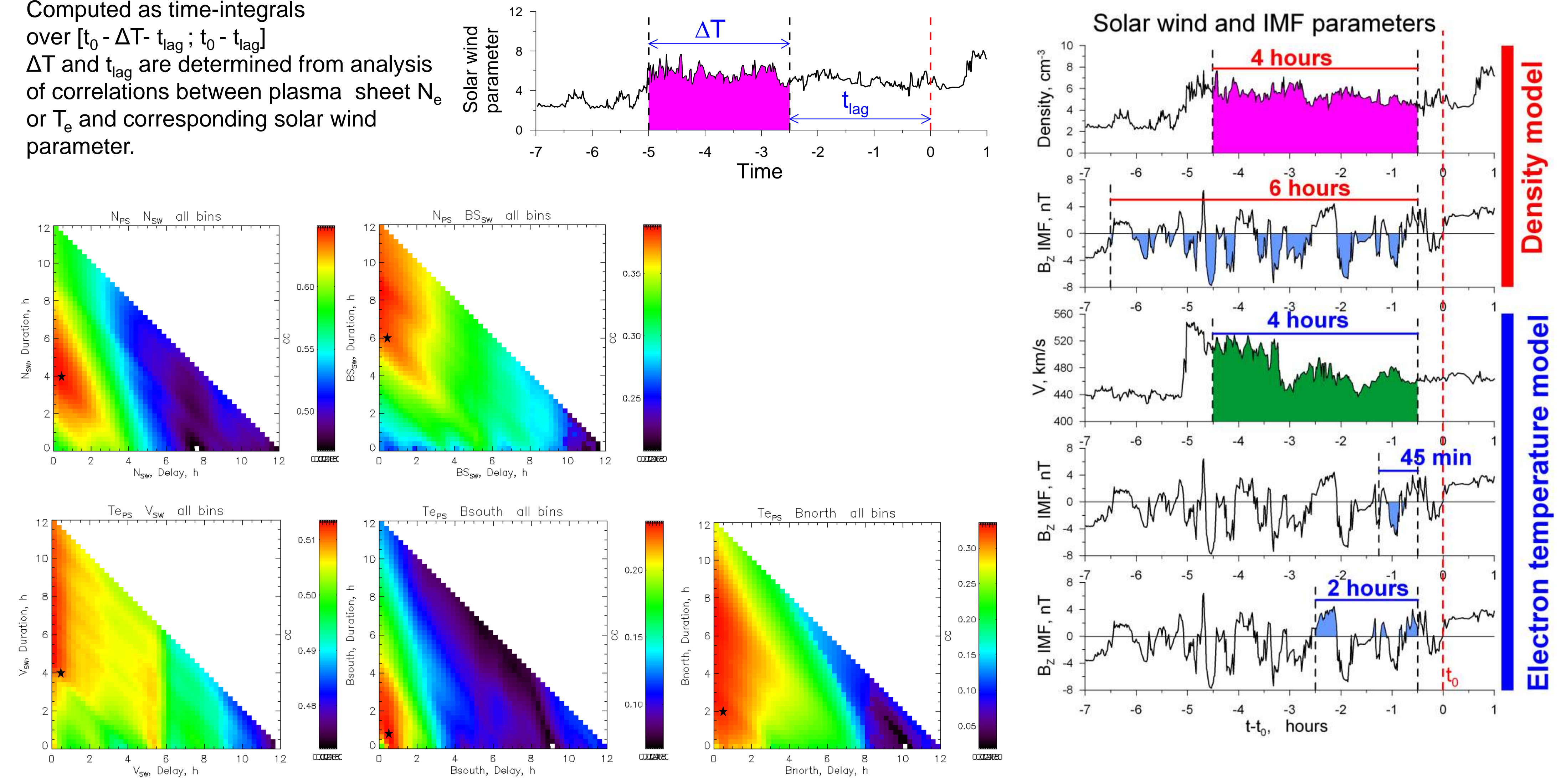
$$N_i / 1.5 < N_e < 1.5 N_i$$

Primary data set: ~45,000 data points (1.6-min res.)



3. Model input parameters

Computed as time-integrals over $[t_0 - \Delta T - t_{lag}; t_0 - t_{lag}]$. ΔT and t_{lag} are determined from analysis of correlations between plasma sheet N_e or T_e and corresponding solar wind parameter.



4. Model equations:

Spatial dependence

$$R = \sqrt{x^2 + y^2 + z^2} \quad \phi = \arctan(-y/x)$$

Normalization

$$N_{SW} = \langle N_{SW} \rangle / 10 \text{ cm}^{-3}$$

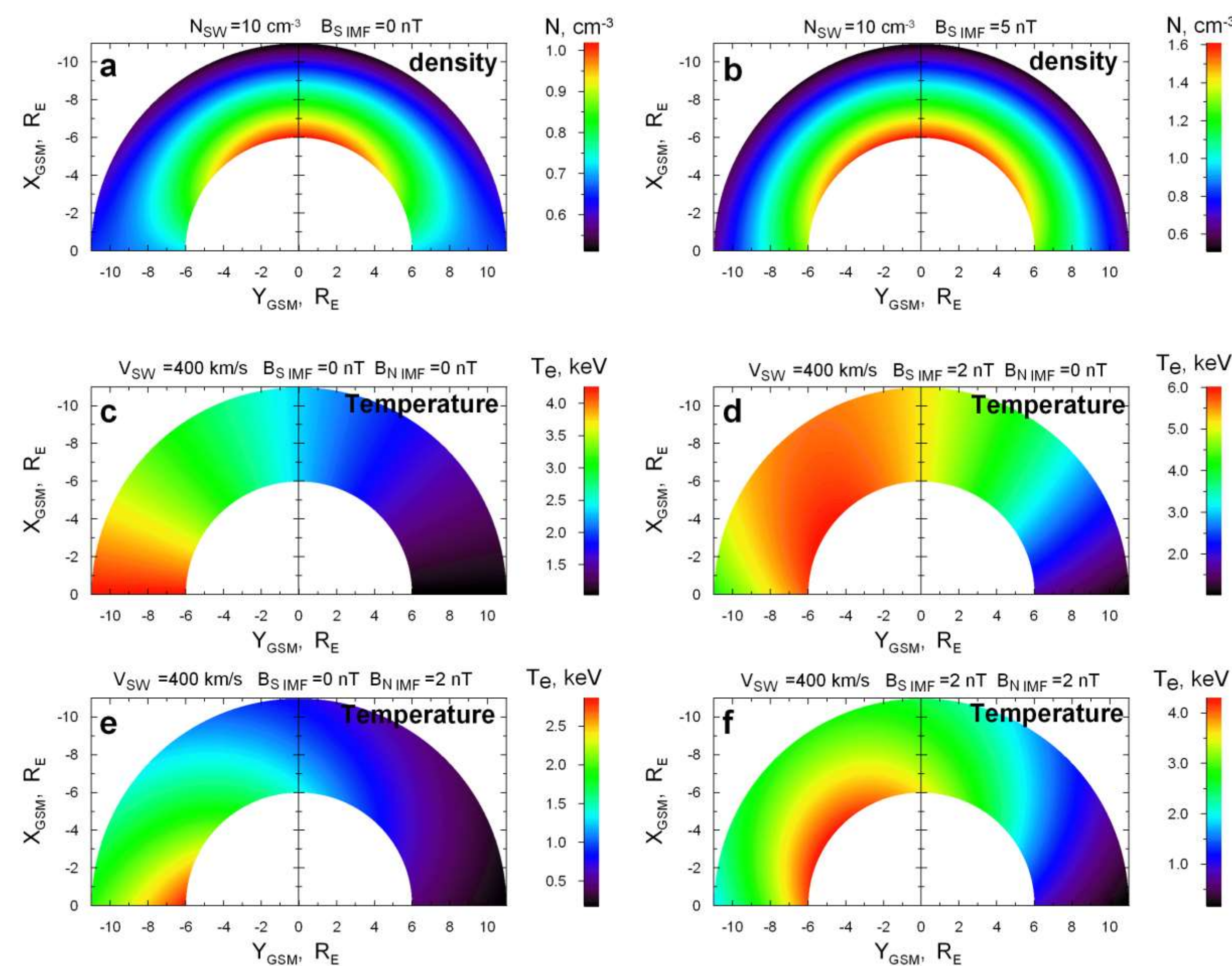
$$V_{SW} = \langle V_{SW} \rangle / 400 \text{ km/s}$$

$$B_S = \langle B_S^{IMF} \rangle / 2 \text{ nT}$$

$$B_N = \langle B_N^{IMF} \rangle / 2 \text{ nT}$$

$$r = R / 10 R_E$$

$$\phi = \phi / 90^\circ$$



Final model equations

Electron density model: 7 coefficients

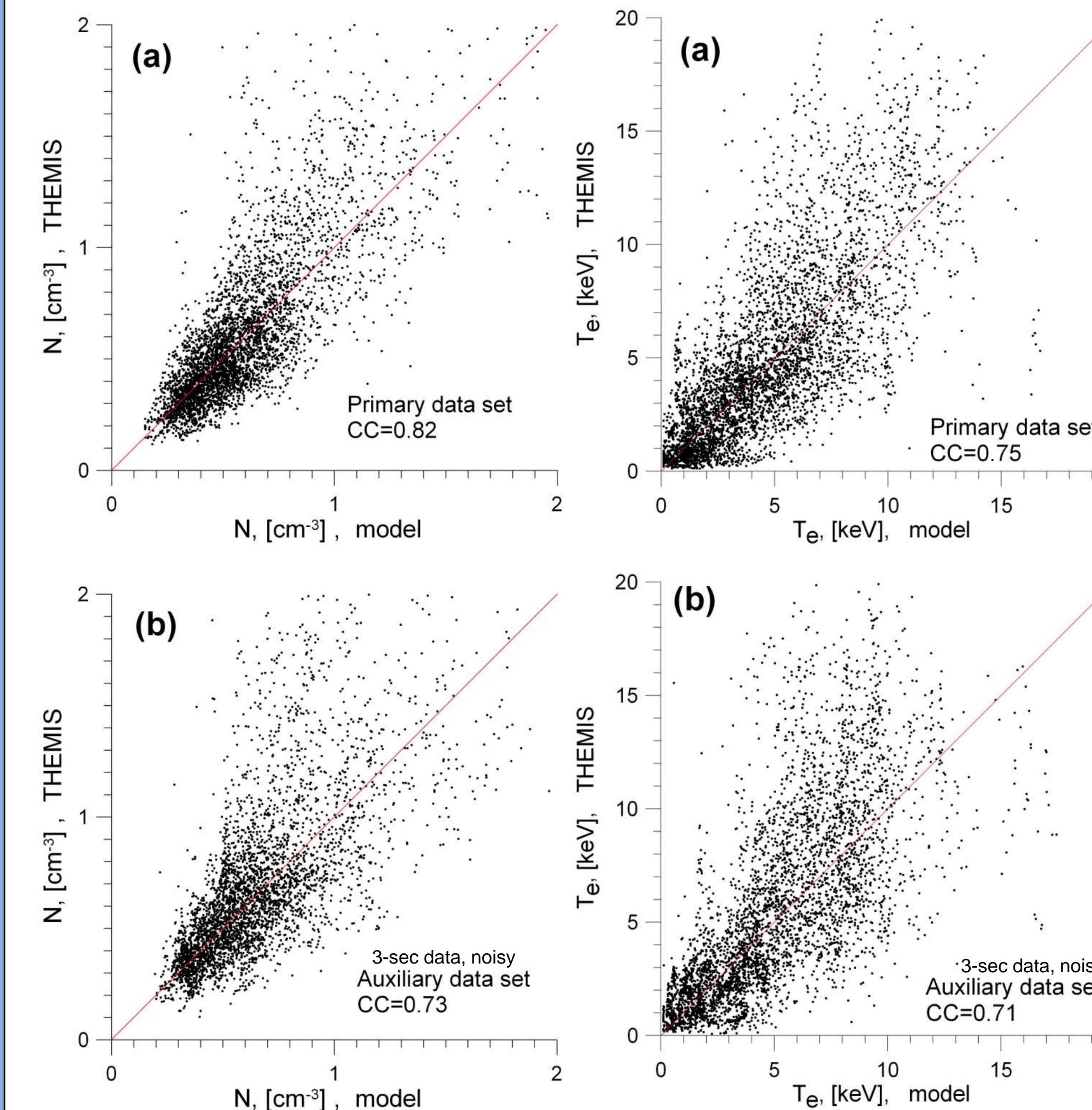
$$N_e = 1.23 - 1.01 \cdot r + 0.874 \cdot r \phi^2 - 0.82 \cdot \phi^2 + 0.392 \cdot N_{SW} + (0.521 - 0.474 \cdot r) \cdot B_S$$

Electron temperature model: 9 coefficients

$$T_e = [-0.0215 - 0.426 \cdot \phi + 0.874 \cdot V_{SW} + (0.587 - 0.538 \cdot r \phi^2) \cdot B_S^{0.32} - 0.489 \cdot r \cdot B_N^{0.36}]^{2.31}$$

5. Model performance

Real data versus model predictions



Primary data set:

3 sec resolution, averaged over 1.6 min, ~45,000 data points

Auxiliary data set:

3 sec resolution, transmitted at 1.6 min resolution, ~12,000 data points

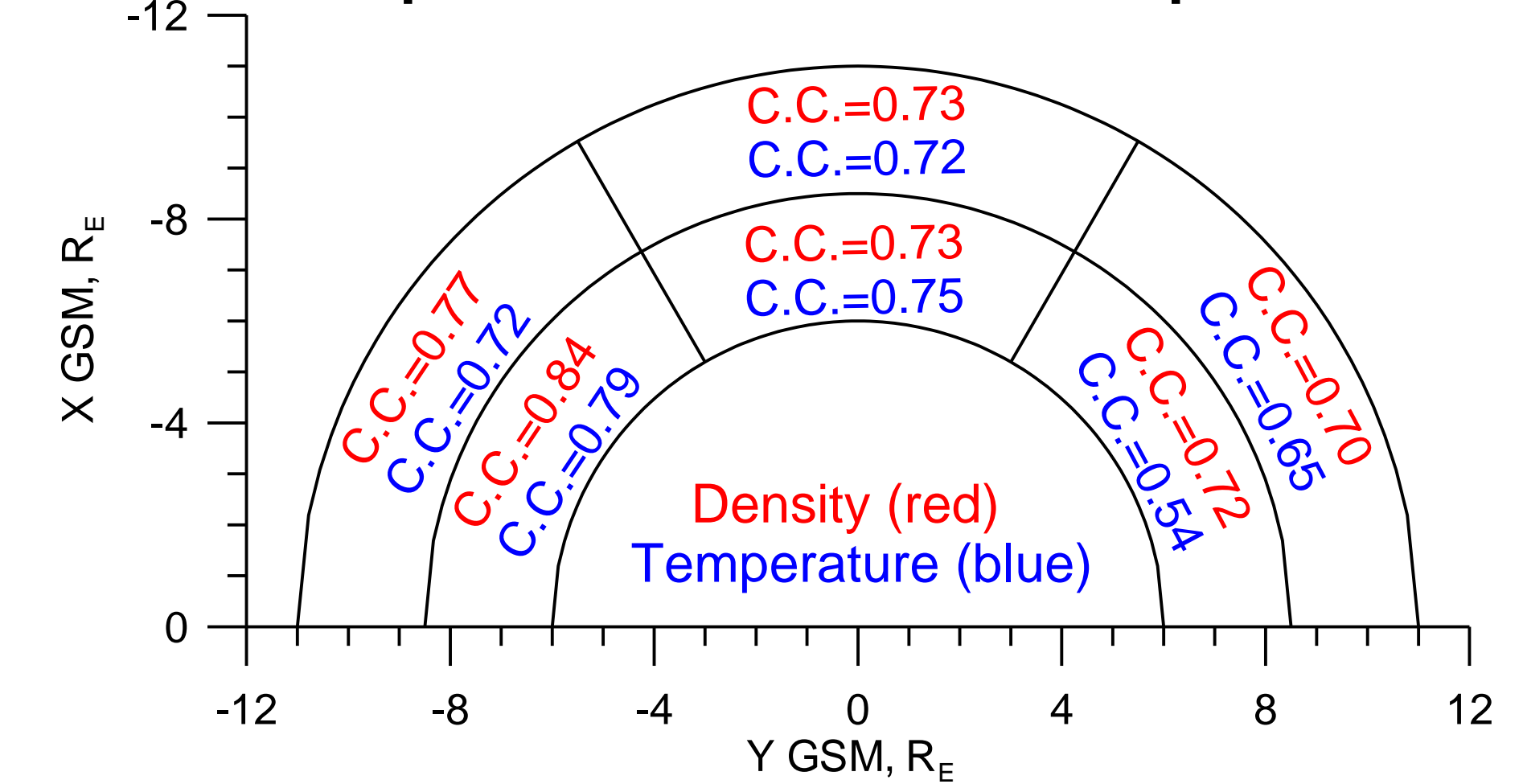
Only 26% of the auxiliary data have "neighbors" from primary data set within ± 30 min.

Results

- The density distribution is symmetric with respect to the midnight meridian, while electron temperature reveals strong azimuthal asymmetry with a maximum in post-midnight MLT sector.
- The electron density dependence on the external driving is parameterized by the solar wind proton density averaged over 4 h and IMF B_S averaged over 6 h. The solar wind proton density is the main controlling parameter, but the IMF B_S becomes of almost the same importance in the near-Earth region.
- The electron temperature model is parameterized by solar wind velocity (averaged over 4 h), IMF B_S (averaged over 45 min), and IMF B_N (averaged over 2 h). The solar wind velocity is a major controlling parameter, and IMF B_S and B_N are comparable in importance. The effect of B_N manifests mostly in the outer part of the modeled region ($r > 8 R_E$). The influence of the IMF B_S is maximal in the midnight to post-midnight MLT sector.
- Both models show very good performance

Density: C.C.=0.82; RMS = 0.23 cm^{-3}
 Temperature: C.C.=0.75; RMS = 2.6 keV

Model performance for different spatial bins



ACKNOWLEDGMENTS:

The projects leading to these results have received funding from the European Union Seventh Framework Programme (FP7/2007-2013) under grant agreement No 606716 SPACESTORM and from the European Union's Horizon 2020 research and innovation program under grant agreement No 637302 PROGRESS

For the full model description see *Dubyagin et al., JGR, 2016*. The model code and subroutines for the input parameter computation are available in supplemental materials of the paper.